Contribution from the Anorganisch Chemisch Laboratorium and Laboratorium voor Kristallografie, University of Amsterdam, 1018 WV Amsterdam, The Netherlands

Ruthenium Carbonyl 1,4-Diaza-1,3-butadiene (R-DAB) Reaction Sequence.[1] Reversible CO Addition to a Trinuclear Species without Rupture of a Metal-Metal Bond. Molecular Structure of [1,4-Dicyclohexyl-1,4-diaza-1,3-butadiene]nonacarbonyltriruthenium, $Ru_3(CO)_9$(c-Hx-DAB): A Unique 50e Trinuclear Compound with Two Elongated Ru-Ru Bonds

JAN KEIJSPER,† LOUIS H. POLM,† GERARD VAN KOTEN,† KEES VRIEZE,*† PAUL F. A. B. SEIGNETTE,‡ and CASPER H. STAM‡

Received March 28, 1984

$Ru_3(CO)_{12}$ reacts with 1,4-disubstituted 1,4-diaza-1,3-butadienes, R-DAB = R—N=C(H)—C(H)=N—R (R = *i*-Pr, c-Hx, *neo*-Pent, *i*-Bu, *p*-Tol), to yield mononuclear $Ru(CO)_3$(R-DAB) as a (c-Hx-DAB)) observable intermediate. This monomer reacts further with $Ru_3(CO)_{12}$ to give known dimeric $Ru_2(CO)_n$(R-DAB) (n = 5, 6) compounds. Dimeric $Ru_2(CO)_6$(c-Hx-DAB) reacts with $Ru_3(CO)_{12}$ to yield novel trinuclear $Ru_3(CO)_9$(c-Hx-DAB), which was characterized by an X-ray crystal structure determination. Crystals of $Ru_3(CO)_9$(c-Hx-DAB) are monoclinic, space group $P2_1/n$ and cell constants a = 11.695 (2) Å, b = 10.306 (2) Å, c = 23.193 (3) Å, β = 102.73 (1)°, and Z = 4. A total of 2968 reflections have been used in the refinement, which results in a final R value of 0.034. In the triangular array of Ru atoms, there are two elongated Ru-Ru distances (Ru(1)-Ru(2) = 3.026 (1) Å, Ru(2)-Ru(3) = 2.956 (1) Å) while the third is normal (Ru(1)-Ru(3) = 2.793 (1) Å). All nine carbonyls are terminally bonded: four to Ru(3), three to Ru(2), and two to Ru(1). The c-Hx-DAB ligand is σ-N,σ-N′ coordinated to Ru(2) with equal, normal Ru-N distances of 2.13 (1) Å (mean). The four atoms of the N(1)=C(1)—C(2)=N(2) skeleton are located equal distances (2.22 (1) Å) (mean) from Ru(1), consistent with η^2 coordination of both double bonds to Ru(1). Also, the bond lengths within this N(1)=C(1)—C(2)=N(2) part are equal (1.39 (1) Å) (mean), indicating that the diimine ligand is in a symmetrical 8e, σ-N,σ-N′,η^2-C=N,η^2-C′=N′ coordination mode. As a consequence, $Ru_3(CO)_9$(c-Hx-DAB) is considered as a 50e - (3 × 8e (Ru) + 9 × 2e (CO) + 8e (c-Hx-DAB)) trinuclear species. Assuming 2e-2c Ru-Ru bonds, the structure does not obey the 18e rule, but it is shown that it can be interpreted on the basis of the polyhedral skeletal electron pair theory (PSEPT). $Ru_3(CO)_9$(R-DAB) (R = *neo*-Pent, *i*-Bu), which have according to spectral data the same geometry as $Ru_3(CO)_9$(c-Hx-DAB), are instaneously formed in the reaction of $Ru_3(CO)_8$(R-DAB) with CO gas in toluene. This reaction can easily be reversed by heating $Ru_3(CO)_9$(R-DAB) in toluene or by treating it with Me_3NO. The traffic light like color change during this reaction, which is reversible, is very remarkable: $Ru_3(CO)_8$(R-DAB) (bright green) + CO ⇄ $Ru_3(CO)_9$(R-DAB) (bright red). Based on a structural comparison between $Ru_3(CO)_8$(R-DAB) and $Ru_3(CO)_9$(R-DAB), a rationale is given for the ease of CO addition, which does not lead to the complete rupture of bonds. Furthermore, the analogy between the reactions of $Fe_2(CO)_9$ and of $Ru_3(CO)_{12}$ with R-DAB is discussed. On the basis of PSEPT, the analogy between the reactions of $Ru_2(CO)_5$(R-DAB) and of isolobal $Ru_3(CO)_8$(R-DAB) with CO is discussed.

Introduction

In the course of our study of the coordination and activation of the 1,4-disubstituted 1,4-diaza-1,3-butadienes, R-DAB = R—N=C(H)—C(H)=N—R on carbonyls of the iron triad ($Fe_2(CO)_9$, $Ru_3(CO)_{12}$, $Os_3(CO)_{12}$), we have isolated many mono- as well as polynuclear species.[2-7] Only for M = Fe, was the reaction route to the different products known in some detail: $Fe_2(CO)_9$ reacts with R-DAB to yield the mononuclear species $Fe(CO)_3$(R-DAB) that can react further with $Fe_2(CO)_9$ to give dinuclear $Fe_2(CO)_6$(R-DAB),[7a] which was first isolated by Fruehauf et al. in 1978.[9]

To explain the different products in the reaction of $M_3(CO)_{12}$ (M = Ru, Os) with R-DAB, another reaction path has been suggested that involves stepwise breakdown of the cluster via $M_3(CO)_{10}$(R-DAB) and $M_3(CO)_9$(R-DAB). The latter species has been observed by FD-MS for M = Os.[7b] Thus, for M = Ru, it was considered a possibility that further reaction of initially formed $Ru_3(CO)_{10}$(R-DAB) would yield either $Ru_3(CO)_8$(R-DAB), $Ru_2(CO)_6$(R-DAB), or $Ru(CO)_3$(R-DAB), depending mainly on the steric properties of R.[2,7b] The recent isolation of $Ru_2(CO)_5$(R-DAB) and the study of its chemistry as well as the observation that $Ru_3(CO)_8$(R-DAB) is actually formed out of $Ru_2(CO)_5$(R-DAB) through reaction with $Ru_3(CO)_{12}$[6] have suggested that $Ru_2(CO)_5$(R-DAB) is the more likely key intermediate in the $Ru_3(CO)_{12}$/(R-DAB) reaction sequence and that for M = Ru the above-mentioned reaction scheme is not correct. Indeed, closer inspection of the initial stages of the reactions of R-DAB with $Ru_3(CO)_{12}$ showed the presence in solution of monomeric $Ru(CO)_3$(R-DAB) as a common intermediate. No evidence for the previously suggested formation of $Ru_3(CO)_{10}$(R-DAB) could be obtained, although it is very likely that the cluster breakdown to yield monomeric $Ru(CO)_3$(R-DAB) is preceded by coordination of R-DAB to the Ru_3 cluster. In this paper we present further evidence for the formation and nature of this mononuclear intermediate in the initial stage of the $Ru_3(CO)_{12}$/R-DAB reaction.

Furthermore, the reversible reaction of $Ru_3(CO)_8$(R-DAB) with CO, leading to $Ru_3(CO)_9$(R-DAB), will be described. This reaction is part of our study of the reactivity of $Ru_3(CO)_8$(R-DAB) toward small molecules such as CO, CH_2N_2, H_2, and acetylenes. Our interest in the chemistry of this trinuclear species was prompted by the recognition of the structural similarity between $Ru_3(CO)_8$(R-DAB) and the very reactive species Ru_2-

† Anorganisch Chemisch Laboratorium.
‡ Laboratorium voor Kristallografie.

(1) Ruthenium Carbonyl 1,4-Diaza-1,3-butadiene Complexes. Part 6. For earlier parts see ref 2-6.
(2) Staal, L. H.; Polm, L. H.; Vrieze, K.; Ploeger, F.; Stam, C. H. *Inorg. Chem.* **1981**, *20*, 3590.
(3) Staal, L. H.; Polm, L. H.; Balk, R. W.; van Koten, G.; Vrieze, K.; Brouwers, A. M. F. *Inorg. Chem.* **1980**, *19*, 3343.
(4) Staal, L. H.; van Koten, G.; Vrieze, K.; van Santen, B.; Stam, C. H. *Inorg. Chem.* **1981**, *20*, 3598.
(5) Staal, L. H.; van Koten, G.; Vrieze, K.; Ploeger, F.; Stam, C. H. *Inorg. Chem.* **1981**, *20*, 1830.
(6) Keijsper, J. J.; Polm, L. H.; van Koten, G.; Vrieze, K.; Abbel, G.; Stam, C. H. *Inorg. Chem.* **1984**, *23*, 2142.
(7) (a) Staal, L. H.; Polm, L. H..; Vrieze, K. *Inorg. Chim. Acta* **1980**, *40*, 165. (b) Staal, L. H.; van Koten, G.; Vrieze, K. *J. Organomet. Chem.* **1981**, *206*, 99. (c) See also ref 2, 3, 6, and 8.
(8) (a) Vrieze, K.; van Koten, G.; Staal, L. H. *Inorg. Chim. Acta* **1982**, *62*, 23. (b) van Koten, G.; Vrieze, K. *Adv. Organomet. Chem.* **1982**, *21*, 151.
(9) Fruehauf, H. W.; Lander, A.; Goddard, R.; Krueger, C. *Angew. Chem.* **1978**, *90*, 56.

0020-1669/85/1324-0518$01.50/0

Table I. IR Data of the First Observed Intermediate in the $Ru_3(CO)_{12}$/R-DAB Reaction

R	obsd freq[a]	R	obsd freq[a]
i-Pr	2036, 1963	*neo*-Pent[b]	2040, 1966
c-Hx	2033, 1963	*p*-Tol[c]	2049, 1973
i-Bu	2038, 1965		
$Ru(CO)_3((i\text{-Pr})_2Me\text{-DAB})$[b]	2034, 1965[d]		

[a] The values (cm^{-1}) have been obtained in heptane solution in the ν(CO) region, after stirring 0.33 mmol of $Ru_3(CO)_{12}$ with 0.5 mmol of R-DAB at 80 °C for 0.5 h. All spectra also showed absorptions at 2057, 2026, and 2009 cm^{-1}, which were assigned to the ν(CO) frequencies of $Ru_3(CO)_{12}$. [b] See also Figure 1. [c] In this reaction, 1.0 mmol of *p*-Tol-DAB is used (solvent toluene). [d] Reported literature values for the isolated monomer.[2]

$(CO)_5$(R–DAB).[6] Both trimeric and dimeric species contain an 8e, σ-N,σ-N′,η^5-C=N,η^5-C′=N′-bonded R–DAB, and they can be described as $[Ru_2(CO)_4(R\text{–}DAB)(\mu\text{-}Ru(CO)_4)]$ and $[Ru_2(CO)_4(R\text{–}DAB)(\mu\text{-}CO)]$, respectively. The reactivity pattern of $Ru_3(CO)_8$(R–DAB), which has striking similarity with that of $Ru_2(CO)_5$(R–DAB), will be discussed in detail in a forthcoming paper.

Experimental Section

Materials and Apparatus. ^1H NMR spectra were obtained on a Varian T60 and a Bruker WM250 spectrometer. IR spectra were recorded with a Perkin-Elmer 283 spectrophotometer. UV–visible measurements were carried out on a Cary 14 spectrometer. Elemental analyses were obtained from the section Elemental Analysis of the Institute for Applied Chemistry, TNO, Utrecht, The Netherlands. All preparations were done in an atmosphere of purified nitrogen, using carefully dried solvents. The R–DAB (R = *i*-Pr, c-Hx, *i*-Bu, *neo*-Pent, *p*-Tol) ligands have been prepared by the condensation reaction of glyoxal with the appropriate amine.[2,10a] $Ru_3(CO)_{12}$ was purchased from Strem Chemicals and used without purification. Me_3NO was prepared according to literature methods.[10b]

Formation of $Ru(CO)_3$(R–DAB) (R = *i*-Pr, c-Hx, *i*-Bu, *neo*-Pent, *p*-Tol). $Ru_3(CO)_{12}$ (0.33 mmol) and R–DAB (0.5 mmol, R = *i*-Pr, c-Hx, *i*-Bu, *neo*-Pent; 1.0 mmol, R = *p*-Tol) were stirred in 30 mL of heptane or toluene at 80 °C for about 0.5 h. The color of the solution changed to blood red, and IR spectroscopy at this stage indicated the presence in solution of $Ru(CO)_3$(R–DAB) and $Ru_3(CO)_{12}$ (see Table I). Further heating of this reaction mixture for 2 h at 110 °C yielded either $Ru_2(CO)_6$(R–DAB) (R = *i*-Pr, c-Hx), $Ru_2(CO)_5$(R–DAB) (R = *i*-Bu, *neo*-Pent), or $Ru_2(CO)_4$(*p*-Tol–DAB)$_2$, which could be isolated as reported earlier.[3,6] When $Ru_3(CO)_{12}$ (0.33 mmol) was reacted with an excess (>2 mmol) of R–DAB (R = *p*-Tol, *i*-Pr, *neo*-Pent, *i*-Bu), IR spectroscopy (Table I) indicated the presence in solution of $Ru(CO)_3$(R–DAB), which upon refluxing reacted only very slowly (>10 h) to $Ru_2(CO)_4$(R–DAB)$_2$. During this reaction no $Ru_2(CO)_n$(R–DAB) (n = 5, 6) was formed, as evidenced by IR spectroscopy.

Syntheses. $Ru_3(CO)_9$(R–DAB) (R = *neo*-Pent, *i*-Bu). A toluene solution (30 mL) of $Ru_3(CO)_8$(R–DAB) (0.33 mmol, prepared in situ)[6] was stirred under a CO atmosphere at room temperature for 5 min. The color of the solution turned from green to red. The toluene was evaporated at 50 °C and the product extracted under a CO atmosphere with 30 mL of hexane. Crystallization at −80 °C resulted in the formation of red crystals (isolated in about 60% yield) that were identified as $Ru_3(CO)_9$(R–DAB) by analysis and IR and ^1H NMR spectroscopies (see Table II). The yield of the complexes in solution was almost quantitative.

$Ru_3(CO)_9$(c-Hx–DAB). $Ru_3(CO)_{12}$ (0.20 mmol) was added to a heptane solution (30 mL) of $Ru_2(CO)_6$(c-Hx–DAB), prepared in situ;[3] the solution was heated at 100 °C for 1.5 h and then filtered hot. The filtrate was slowly cooled to −20 °C, resulting in the precipitation of red crystals that were isolated in about 30% yield (based on c-Hx–DAB) and were identified as $Ru_3(CO)_9$(c-Hx–DAB) by analysis, IR and ^1H NMR spectroscopy (Table II), and an X-ray structure determination.

Crystal Structure Determination of $Ru_3(CO)_9$(c-Hx–DAB), $C_{23}H_{24}N_2O_9Ru_3$, Nonacarbonyl[1,4-dicyclohexyl-1,4-diaza-1,3-butadiene]triruthenium. Crystals of the title compound were brick shaped, monoclinic, space group $P2_1/n$. The unit cell had the dimensions a = 11.695 (2) Å, b = 10.306 (2) Å, c = 23.193 (3) Å, β = 102.73 (1)°, Z = 4, V = 2726.7 Å^3, d_{calcd} = 1.89 g cm^{-3}. A total of 2968 independent reflections ($-13 \leq h \leq 13$, $0 \leq k \leq 12$, $0 \leq l \leq 20$) with intensities above the $2.5\sigma(I)$ level were measured at room temperature, on a Nonius CAD 4 diffractometer, using graphite-monochromated Mo Kα radiation ($2\theta < 50°$, λ = 0.71069 Å). The total number of accessible independent reflections was 4800. Application of the symbolic addition program set SIMPEL[11] revealed the presence of three Ru atoms in the asymmetric unit. From a subsequent Fourier synthesis the remaining non-hydrogen atoms were derived. After isotropic block-diagonal least-squares refinement, an empirical absorption correction was applied[12a] (crystal dimensions 0.07 × 0.12 × 0.25 mm; μ = 16.60 cm^{-1}). Subsequent anisotropic refinement converged to R = 0.034 (R_w = 0.038). During the final cycles, the H atoms, which were

Table II. Spectroscopic Data of $Ru_3(CO)_9$(R–DAB)

R in $Ru_3(CO)_9$-(R–DAB)	ν(CO)[a]	^1H NMR chem shifts[b] R group	^1H NMR chem shifts[b] imine H
c-Hx[c]	2075 2034 1998 1984 1971 1933	2.09 (1 H, m), 2.1 (10 H, m)	5.30 (1 H, s)
neo-Pent	2077 2036 1998 1985 1975 1939	3.21 (1 H, d, J = 13 Hz)|2.02 (1 H, d, J = 13 Hz), 1.01 (9 H, s)	5.41 (1 H, s)
i-Bu	2075 2034 1997 1984 1972 1938	3.23 (1 H, d[d] of d[e])|1.76 (1 H, m), 1.85 (1 H, m), 0.87 (3 H, d, J = 6 Hz)|0.82 (3 H, d, J = 6 Hz)	5.19 (1 H, s)

compd	elec abs max, nm (ϵ)[f]	color
$Ru_3(CO)_8$(*neo*-Pent–DAB)	680 (1600), 440 (2500), 380 (740)	green
$Ru_3(CO)_9$(*neo*-Pent–DAB)	460 (2500), 340 (560)	red

[a] In hexane solution. [b] In toluene-d_8 solution; shifts in ppm relative to Me_4Si; vertical bars to separate diastereotopic pairs; d = doublet, s = singlet, m = multiplet. [c] Poorly soluble in hexane; ν(CO) frequencies in dichloromethane solution are 2074, 2033, 1996, 1985 (sh), 1968, and 1920 cm^{-1}. [d] J = 3 Hz. [e] J = 13 Hz. [f] In toluene solution at room temperature; ϵ in L mol^{-1} cm^{-1}.

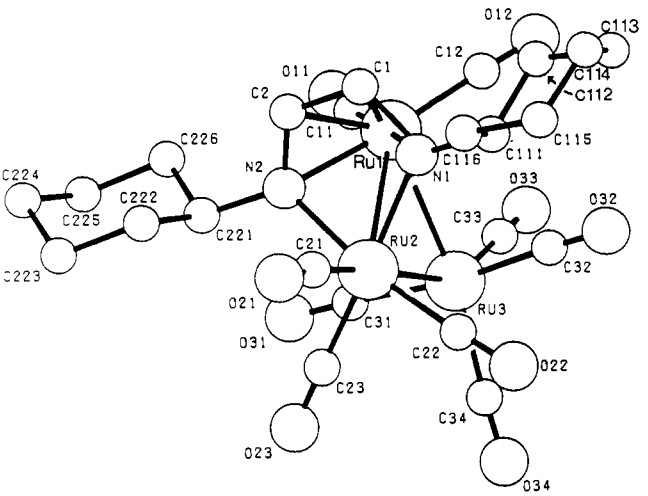

Figure 1. Molecular geometry of $Ru_3(CO)_9$(c-Hx–DAB).

(10) (a) Kliegman, J. M.; Barnes, R. K. *J. Organomet. Chem.* **1970**, *35*, 3140. (b) Lecher, H. Z.; Hardy, W. B. *J. Am. Chem. Soc.* **1948**, *70*, 3789.

(11) Overbeek, A. R.; Schenk, H. "Computing in Crystallography"; Delft University Press: Delft, 1978.

(12) (a) Walker, N.; Stuart, D. *Acta Crystallogr., Sect. A: Found. Crystallogr.* **1983**, *A39*, 158. (b) "International Tables for Crystallography"; Kynoch Press: Birmingham, England, 1974; Vol. IV. (c) Motherwell, S.; Clegg, B. "PLUTO, Program for Plotting Molecular and Crystal Structures"; University of Cambridge: Cambridge, England, 1978.

Table III. Final Atomic Coordinates (with Esd's in Parentheses) of $Ru_3(CO)_9$(c-Hx-DAB)

	x	y	z
Ru1	0.15443 (5)	0.43374 (6)	0.44125 (3)
Ru2	0.11352 (5)	0.19982 (6)	0.36049 (3)
Ru3	0.27389 (6)	0.41567 (7)	0.34970 (3)
C1	0.0758 (7)	0.2696 (8)	0.4799 (4)
C2	−0.0129 (6)	0.3357 (8)	0.4417 (4)
C11	0.1225 (7)	0.6095 (9)	0.4281 (4)
C12	0.2821 (8)	0.4909 (9)	0.4990 (4)
C21	0.0104 (7)	0.0554 (8)	0.3625 (4)
C22	0.2404 (7)	0.0931 (9)	0.3501 (4)
C23	0.0711 (7)	0.2245 (8)	0.2778 (4)
C31	0.1403 (9)	0.5041 (9)	0.3014 (5)
C32	0.3872 (8)	0.3160 (10)	0.4055 (5)
C33	0.3556 (9)	0.5768 (11)	0.3763 (5)
C34	0.3309 (8)	0.3641 (10)	0.2817 (5)
C111	0.2507 (7)	0.1331 (8)	0.4934 (4)
C112	0.3117 (8)	0.1906 (10)	0.5516 (4)
C113	0.4002 (9)	0.0936 (10)	0.5875 (4)
C114	0.3445 (8)	−0.0342 (10)	0.5947 (4)
C115	0.2822 (9)	−0.0913 (9)	0.5354 (5)
C116	0.1940 (8)	0.0035 (8)	0.5015 (4)
C221	−0.1064 (7)	0.3955 (8)	0.3421 (4)
C222	−0.2062 (7)	0.2989 (9)	0.3323 (4)
C223	−0.3108 (8)	0.3451 (10)	0.2863 (5)
C224	−0.3522 (8)	0.4759 (10)	0.3031 (5)
C225	−0.2512 (9)	0.5742 (10)	0.3108 (4)
C226	−0.1465 (8)	0.5285 (9)	0.3580 (5)
N1	0.1630 (5)	0.2186 (6)	0.4538 (3)
N2	−0.0016 (5)	0.3410 (6)	0.3838 (3)
O11	0.1071 (6)	0.7191 (6)	0.4227 (4)
O12	0.3591 (7)	0.5312 (8)	0.5342 (3)
O21	−0.0480 (6)	−0.0333 (6)	0.3597 (3)
O22	0.3162 (6)	0.0287 (8)	0.3446 (3)
O23	0.0442 (7)	0.2396 (8)	0.2274 (3)
O31	0.0653 (6)	0.5573 (8)	0.2713 (4)
O32	0.4577 (6)	0.2627 (8)	0.4382 (4)
O33	0.4022 (8)	0.6693 (9)	0.3934 (4)
O34	0.3676 (7)	0.3395 (9)	0.2405 (4)
H1	0.084 (4)	0.253 (5)	0.518 (2)
H2	−0.085 (5)	0.369 (6)	0.453 (3)
H111	0.303 (5)	0.110 (5)	0.472 (2)
H1121	0.357 (9)	0.269 (10)	0.556 (5)
H1122	0.256 (7)	0.199 (9)	0.573 (4)
H1131	0.464 (6)	0.088 (8)	0.557 (3)
H1132	0.440 (8)	0.135 (9)	0.618 (4)
H1141	0.411 (9)	−0.103 (11)	0.629 (5)
H1142	0.289 (9)	−0.034 (11)	0.626 (5)
H1151	0.352 (9)	−0.109 (11)	0.513 (5)
H1152	0.253 (7)	−0.165 (8)	0.539 (4)
H1161	0.160 (6)	−0.034 (8)	0.466 (3)
H1162	0.117 (6)	0.018 (7)	0.524 (3)
H221	−0.081 (5)	0.398 (6)	0.309 (3)
H2221	−0.179 (7)	0.234 (9)	0.314 (4)
H2222	−0.228 (7)	0.298 (8)	0.374 (4)
H2231	−0.302 (6)	0.353 (7)	0.245 (3)
H2232	−0.388 (10)	0.264 (12)	0.279 (5)
H2241	−0.410 (7)	0.504 (8)	0.272 (4)
H2242	−0.362 (12)	0.498 (14)	0.358 (6)
H2251	−0.247 (5)	0.568 (6)	0.268 (3)
H2252	−0.268 (8)	0.655 (9)	0.325 (4)
H2261	−0.081 (6)	0.592 (7)	0.357 (3)
H2262	−0.178 (8)	0.529 (9)	0.400 (4)

indicated in a ΔF synthesis, were included with isotropic temperature parameters. Unit weights were applied, and the anomalous scattering of Ru was taken into account.[12b] No extinction correction was applied. The computer programs used for plotting,[12c] the scattering factors, and the dispersion correction[12b] were taken from the literature.

The molecular geometry of $Ru_3(CO)_9$(c-Hx-DAB) with the numbering of the atoms is shown in Figure 1, which shows a PLUTO[12c] drawing of the molecule. Atomic parameters, bond lengths, and selected bond angles are given in Tables III, IV, and V, respectively. All bond angles, anisotropic thermal parameters, and a list of observed and calculated structure factors are included with the supplementary material.

CO Elimination from $Ru_3(CO)_9$(R–DAB) (R = *i*-Bu, *neo*-Pent). By Heating. A toluene solution of $Ru_3(CO)_9$(R–DAB) was refluxed for 2 h during which time the color of the solution changed from red to green.

Table IV. Bond Distances (with Esd's in Parentheses) in Å within $Ru_3(CO)_9$(c-Hx-DAB)

	Metal–Carbonyl		
Ru(1)–Ru(2)	3.026 (1)		
Ru(1)–Ru(3)	2.793 (1)	C(11)–O(11)	1.146 (11)
Ru(2)–Ru(3)	2.956 (1)	C(12)–O(12)	1.152 (11)
Ru(1)–C(11)	1.861 (9)	C(21)–O(21)	1.134 (11)
Ru(1)–C(12)	1.868 (8)	C(22)–O(22)	1.137 (12)
Ru(2)–C(21)	1.923 (8)	C(23)–O(23)	1.152 (11)
Ru(2)–C(22)	1.905 (9)	C(31)–O(31)	1.135 (12)
Ru(2)–C(23)	1.889 (9)	C(32)–O(32)	1.132 (12)
Ru(3)–C(31)	1.938 (10)	C(33)–O(33)	1.126 (14)
Ru(3)–C(32)	1.931 (10)	C(34)–O(34)	1.159 (15)
Ru(3)–C(33)	1.947 (11)		
Ru(3)–C(34)	1.918 (12)		
	Metal–c-Hx–DAB		
Ru(1)–N(1)	2.236 (6)	Ru(1)–C(2)	2.204 (8)
Ru(1)–N(2)	2.224 (6)	Ru(2)–N(1)	2.122 (7)
Ru(1)–C(1)	2.208 (9)	Ru(2)–N(2)	2.131 (7)
	c-Hx–DAB		
C(1)–C(2)	1.386 (11)	C(115)–C(116)	1.510 (13)
C(1)–N(1)	1.398 (12)	C(116)–C(111)	1.521 (12)
C(2)–N(2)	1.379 (12)	C(221)–C(222)	1.513 (12)
N(1)–C(111)	1.502 (10)	C(222)–C(223)	1.512 (12)
N(2)–C(221)	1.494 (10)	C(223)–C(224)	1.512 (15)
C(111)–C(112)	1.503 (12)	C(224)–C(225)	1.536 (14)
C(112)–C(113)	1.544 (13)	C(225)–C(226)	1.526 (13)
C(113)–C(114)	1.495 (15)	C(226)–C(221)	1.520 (13)
C(114)–C(115)	1.526 (14)		

$Ru_3(CO)_8$(R–DAB) could be isolated in nearly quantitative yield and was characterized as described earlier.[6] For R = c-Hx, the formation of $Ru_3(CO)_8$(c-Hx–DAB) was demonstrated by IR spectroscopy but it could not be isolated.

By Reaction with Me_3NO. A toluene solution of $Ru_3(CO)_9$(R–DAB) was treated with an equimolar amount of Me_3NO, dissolved in 0.5 mL of CH_2Cl_2. The color of the solution changed immediately from red to green, and $Ru_3(CO)_8$(R–DAB) could be isolated in nearly quantitative yield as described earlier.[6]

Reversibility of CO Addition to $Ru_3(CO)_8$(R–DAB) (R = *i*-Bu, *neo*-Pent). $Ru_3(CO)_9$(R–DAB), dissolved in toluene, was applied to a silica layer. The resulting red spot became green under vacuum but went red again when placed in a CO atmosphere. This procedure could be repeated several times (>10) without noticeable decomposition of the cluster.

Analytical Data. All new complexes gave satisfactory results (supplementary material). The complexes showed characteristic ν(CO) IR absorptions, which are listed in Table I for $Ru(CO)_3$(R–DAB) and Table II for $Ru_3(CO)_9$(R–DAB).

Results

Reaction of $Ru_3(CO)_{12}$ with R–DAB. First Intermediate Observed. When 0.33 mmol of $Ru_3(CO)_{12}$ is reacted with R–DAB (0.5 mmol, R = *i*-Pr, c-Hx, *i*-Bu, *neo*-Pent; 1.0 mmol, R = *p*-Tol) at 80 °C in toluene or heptane for about 0.5 h, a blood red solution is obtained. At this stage in the reaction, IR spectroscopy in the ν(CO) region reveals the presence of both $Ru_3(CO)_{12}$ and another carbonyl species that could not be isolated. The latter compound shows ν(CO) absorptions at about 2035 and 1965 cm^{-1} (see Table I), pointing to mononuclear $Ru(CO)_3$(R–DAB) (see Discussion). Upon further reaction at 110 °C, the IR peaks, ascribed to $Ru(CO)_3$(R–DAB) disappear (vide infra).

When 0.33 mmol of $Ru_3(CO)_{12}$ is reacted with 1.0 mmol of $(i\text{-Pr})_2$Me–DAB, the initial intense red of the solution remains. From this solution $Ru(CO)_3((i\text{-Pr})_2$Me–DAB) can be isolated and characterized by elemental analysis, IR spectroscopy, ^1H NMR, and FD-MS.[2]

The ν(CO) region in the IR spectrum of a heptane solution of this complex reveals two peaks at 2040 and 1969 cm^{-1}. In Figure 4 (supplementary material) this part of the IR spectrum is compared with that of the heptane solution obtained after reacting *neo*-Pent–DAB (0.5 mmol) for 0.5 h with $Ru_3(CO)_{12}$ (0.33 mmol) at 80 °C.

Formation Reactions. Dimeric $Ru_2(CO)_n$(R–DAB) (n = 5, 6). When the blood red solution, containing both $Ru_3(CO)_{12}$ and $Ru(CO)_3$(R–DAB) (vide supra) was heated, $Ru_2(CO)_6$(R–DAB)

Table V. Selected Bond Angles (with Esd's in Parentheses) in deg within $Ru_3(CO)_9$(c-Hx–DAB)

	Within Metal-Carbonyl		
Ru(2)-Ru(1)-Ru(3)	60.89 (3)	Ru(1)-Ru(3)-Ru(2)	63.44 (3)
Ru(1)-Ru(2)-Ru(3)	55.66 (2)	Ru-C-O(mean)[a]	177.1 (15)
	Within Metal-c-Hx-DAB		
Ru(1)-N(1)-Ru(2)	87.9 (2)	Ru(2)-N(2)-C(2)	114.9 (5)
Ru(1)-N(2)-Ru(2)	88.0 (2)	Ru(1)-C(1)-N(1)	72.8 (5)
Ru(2)-N(1)-C(1)	114.5 (5)	Ru(1)-C(2)-N(2)	72.6 (4)
	Within c-Hx-DAB		
C-C-C(c-Hx ring) (mean)[a]	111.1 (7)	C(1)-N(1)-C(111)	114.9 (7)
N(1)-C(1)-C(2)	115.0 (8)	C(2)-N(2)-C(221)	113.9 (6)
C(1)-C(2)-N(2)	115.0 (7)		
	Around Ru(2)		
N(1)-Ru(2)-N(2)	74.0 (2)	C(22)-Ru(2)-C(23)	89.3 (4)
Ru(3)-Ru(2)-C(21)	176.2 (3)	C(22)-Ru(2)-N(1)	97.9 (3)
Ru(3)-Ru(2)-C(22)	84.1 (3)	C(22)-Ru(2)-N(2)	168.4 (3)
Ru(3)-Ru(2)-C(23)	80.9 (3)	C(23)-Ru(2)-N(1)	167.0 (3)
Ru(3)-Ru(2)-N(1)	89.0 (2)	C(23)-Ru(2)-N(2)	97.3 (3)
Ru(3)-Ru(2)-N(2)	87.5 (2)	Ru(1)-Ru(2)-C(21)	128.0 (3)
C(21)-Ru(2)-C(22)	93.8 (4)	Ru(1)-Ru(2)-C(22)	121.1 (3)
C(21)-Ru(2)-C(23)	95.9 (4)	Ru(1)-Ru(2)-C(23)	119.4 (3)
C(21)-Ru(2)-N(1)	94.4 (3)	Ru(1)-Ru(2)-N(1)	47.6 (2)
C(21)-Ru(2)-N(2)	95.0 (3)	Ru(1)-Ru(2)-N(2)	47.3 (2)
	Around Ru(1)		
N(1)-Ru(1)-N(2)	70.1 (2)	N(2)-Ru(1)-Ru(3)	90.0 (2)
C(1)-Ru(1)-C(2)	36.6 (3)	C(12)-Ru(1)-C(11)	84.9 (4)
N(1)-Ru(1)-C(12)	102.3 (3)	C(12)-Ru(1)-Ru(3)	96.4 (3)
N(1)-Ru(1)-C(11)	171.2 (3)	C(11)-Ru(1)-Ru(3)	93.2 (3)
N(1)-Ru(1)-Ru(3)	91.0 (2)	Ru(2)-Ru(1)-C(1)	67.5 (2)
N(2)-Ru(1)-C(12)	170.3 (3)	Ru(2)-Ru(1)-C(2)	67.6 (2)
N(2)-Ru(1)-C(11)	102.2 (3)		
	Around Ru(3)		
Ru(1)-Ru(3)-C(31)	86.2 (4)	Ru(2)-Ru(3)-C(34)	101.7 (3)
Ru(1)-Ru(3)-C(32)	84.9 (4)	C(31)-Ru(3)-C(32)	169.8 (5)
Ru(1)-Ru(3)-C(33)	89.7 (3)	C(31)-Ru(3)-C(33)	93.4 (4)
Ru(1)-Ru(3)-C(34)	165.1 (3)	C(31)-Ru(3)-C(34)	92.1 (5)
Ru(2)-Ru(3)-C(31)	87.5 (3)	C(32)-Ru(3)-C(33)	91.4 (4)
Ru(2)-Ru(3)-C(32)	84.1 (3)	C(32)-Ru(3)-C(34)	95.3 (5)
Ru(2)-Ru(3)-C(33)	153.0 (4)	C(33)-Ru(3)-C(34)	105.2 (5)

[a] The standard deviations of the mean values have been estimated by $\sigma = \{\Sigma_i(x_i - \bar{x})^2/(N-1)\}^{1/2}$.

Scheme I

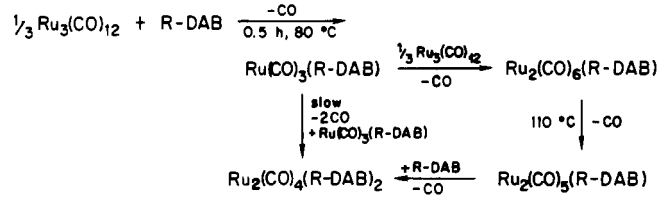

(R = c-Hx, *i*-Pr) and eventually $Ru_2(CO)_5$(R–DAB) (R = c-Hx, *i*-Pr, *neo*-Pent, *i*-Bu) are formed. The formation of these dinuclear species, which can be easily isolated, is indicated by IR spectroscopy (ν(CO) region) and by the color change of the solution from red to red-orange.

When free $Ru_3(CO)_{12}$ is absent, a large excess of R–DAB (R = *i*-Pr, c-Hx, *neo*-Pent, *i*-Bu) is used, or the case of the reaction with *p*-Tol–DAB is being considered, the blood red solution of $Ru(CO)_3$(R–DAB) reacts slowly further, probably via a dimerization reaction, to yield $Ru_2(CO)_4(R–DAB)_2$. This latter product can also be obtained from the reaction of $Ru_2(CO)_5$(R–DAB) with R–DAB[6] for R = *i*-Pr, c-Hx, *neo*-Pent, *i*-Bu. On the basis of these observations Scheme I is proposed (see also Figure 2).

Trinuclear $Ru_3(CO)_n$(R–DAB) (n = 8, 9). $Ru_2(CO)_5$(R–DAB) (R = neo-Pent, *i*-Bu) reacts with $Ru_3(CO)_{12}$ to give green $Ru_3(CO)_8$(R–DAB) in a reaction sequence that probably proceeds via $Ru_3(CO)_9$(R–DAB).[6] CO elimination from this latter species at 110 °C yields the octacarbonyl species. This reaction step can easily be reversed by the reaction of $Ru_3(CO)_8$(R–DAB) with CO

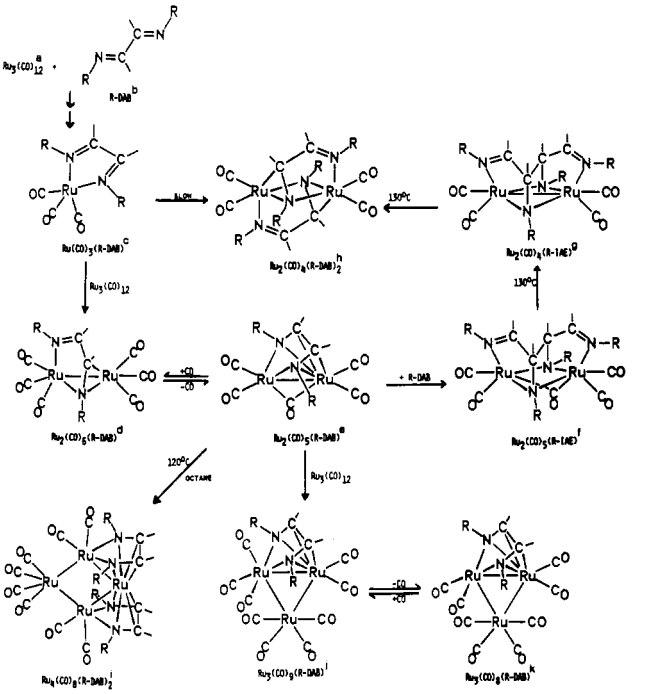

Figure 2. Complete $Ru_3(CO)_{12}$/R–DAB reaction sequence. The superscripts a–k refer to ref 17a–k.

at room temperature, yielding $Ru_3(CO)_9$(R–DAB) quantitatively. Thus, the reaction scheme can be written

$$Ru_2(CO)_5(R–DAB) \xrightarrow[110\ °C]{^1/_3 Ru_3(CO)_{12}} Ru_3(CO)_9(R–DAB) \underset{+CO,\ 110\ °C}{\overset{-CO}{\rightleftharpoons}} Ru_3(CO)_8(R–DAB)$$

red green

$Ru_3(CO)_9$(c-Hx–DAB) is formed in the reaction of $Ru_2(CO)_6$(c-Hx–DAB) with $Ru_3(CO)_{12}$ at 100 °C. At that temperature, however, $Ru_2(CO)_6$(c-Hx–DAB) eliminates CO quite easily to give $Ru_2(CO)_5$(c-Hx–DAB), so this last species is probably the real reagent in the formation reaction of $Ru_3(CO)_9$(c-Hx–DAB). Reaction of $Ru_2(CO)_5$(c-Hx–DAB) with $Ru_3(CO)_{12}$ can be accomplished in a toluene solution at 100 °C, yielding only a small amount of $Ru_3(CO)_9$(c-Hx–DAB) (<5%) because of extensive decomposition. Refluxing $Ru_3(CO)_9$(c-Hx–DAB) in toluene results in a greenish solution, presumably due to $Ru_3(CO)_8$(c-Hx–DAB), but decomposition is complete within 4 h. The following reaction equation is in line with these observations:

$$Ru_2(CO)_6(c\text{-}Hx–DAB) \underset{+CO}{\overset{-CO,\ 100\ °C}{\rightleftharpoons}} Ru_2(CO)_5(c\text{-}Hx–DAB) \xrightarrow[100\ °C]{^1/_3 Ru_3(CO)_{12}}$$

$$Ru_3(CO)_9(c\text{-}Hx–DAB) \xrightarrow[-CO]{100\ °C} Ru_3(CO)_8(c\text{-}Hx–DAB) \rightarrow \text{decompn}$$

IR Spectroscopy (ν(CO) Region). The new $Ru_3(CO)_9$(R–DAB) complexes have a characteristic ν(CO) absorption spectrum (see Table II). They show six intense absorptions in the terminal region only (between 2080 and 1930 cm^{-1}).

FD-MS Spectroscopy. FD-MS, which is often an excellent method for the characterization of new compounds,[13] does not provide spectra in the case of $Ru_3(CO)_9$(R–DAB) showing the

(13) (a) Staal, L. H.; van Koten, G.; Fokkens, R. H.; Nibbering, N. M. M. *Inorg. Chim. Acta* **1981**, *50*, 205. (b) The comments on this structure that we made earlier[8b] were premature: the asymmetry in bonding mode of the c-Hx–DAB ligand, which we thought was present, disappeared as a result of further refinement and application of absorption correction.

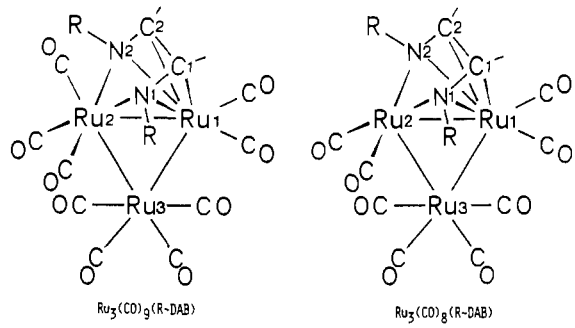

COMPOUND	Ru(1)-Ru(2)	Ru(2)-Ru(3)	Ru(1)-Ru(3)	Ru(1)-C(O)	Ru(2)-C(O)	Ru(3)-C(O)
$Ru_3(CO)_9$(c-Hex-DAB)	3.026(1)	2.956(1)	2.793(1)	1.86(1)	1.91(1)	1.93(1)
$Ru_3(CO)_8$(neo-Pent-DAB)	2.825(1)	2.768(1)	2.737(1)	1.86(1)	1.83(1)	1.93(1)

N(1)-C(1)	N(2)-C(2)	C(1)-C(2)
1.40(1)	1.38(1)	1.39(1)
1.41(1)	1.37(1)	1.39(1)

Figure 3. Schematic structures of $Ru_3(CO)_n$(R–DAB) (n = 8; R = *neo*-Pent;[15] n = 9, R = c-Hx) with relevant geometric properties. The Ru(n)–C(O) (n = 1–3) values are the average Ru–C(carbonyl) distances with standard deviations σ estimated by $\sigma = \{\sum_i(x_i - \bar{x})^2/(N-1)\}^{1/2}$. The Ru–N and Ru–C distances in the nonacarbonyl species tend to be somewhat smaller than the analogous distances in the octacarbonyl species.

molecular ions. $Ru_3(CO)_9$(R–DAB) (R = *i*-Bu, *neo*-Pent) give spectra similar to those of the $Ru_2(CO)_8$(R–DAB) complexes, and $Ru_3(CO)_9$(c-Hx–DAB) gives a mass spectrum in which an isotopic pattern around m/z 750 [highest peak m/z 749 ~ $Ru_3(CO)_8$(c-Hx–DAB)] is observed. These results indicate that the $Ru_3(CO)_9$(R–DAB) compounds produce only $[M - CO]^{+\cdot}$ ions, which is in line with the observed rapid CO dissociation from $Ru_3(CO)_9$(R–DAB) (vide supra).

^{1}H NMR Spectroscopy. The ^{1}H NMR data of $Ru_3(CO)_9$(R–DAB) are listed in Table II. Both imine protons of $Ru_3(CO)_9$(R–DAB) give one singlet at about 5.3 ppm, and also the two R groupings give rise to a single pattern, proving that in solution the geometry of the R–DAB ligand is the same as that in the solid state for R = c-Hx and that a symmetrical 8e coordination mode is present.[2,5,6,8b]

UV–Visible Spectroscopy. A solution of $Ru_3(CO)_9$(*neo*-Pent–DAB) is red, and its absorption in the visible and near-UV regions is compared with those of a $Ru_3(CO)_8$(*neo*-Pent–DAB) solution in Table II. The green of $Ru_3(CO)_8$(*neo*-Pent–DAB) arises from the broad absorption found at 680 nm. Addition of a CO group to $Ru_3(CO)_8$(*neo*-Pent–DAB) causes a complete disappearance of this 680-nm absorption while the other parts of the UV spectra of the two trimeric species are comparable. It can be seen from Figure 3 that addition of a CO group to $Ru_3(CO)_8$(*neo*-Pent–DAB) takes place on the Ru(2) atom to which the diimine ligand is σ-N,σ-N′ coordinated (vide infra), while the coordination spheres of the other Ru atoms are not drastically changed on going from the octa- to the nonacarbonyl. Therefore, one may tentatively assign the absorption at 680 nm to a LF transition localized on the Ru(2) atom. Addition to this Ru(2) atom of a CO ligand, whose carbon lone pair probably has a strong interaction with the highest unfilled ligand field state on Ru(2), then causes a shift of the 680-nm transition to the UV region. The remaining weak absorptions at about 450 and 360 nm are likely to be due to LF transitions localized on the other Ru atoms.

Molecular Geometry of $Ru_3(CO)_9$(c-Hx–DAB). The molecular geometry[13b] of $Ru_3(CO)_9$(c-Hx–DAB) together with the atomic numbering is shown in Figure 1. In Tables III, IV, and V the atomic coordinates, bond lengths, and important bond angles are given.

Two Ru–Ru separations in the triangular array of Ru atoms may be envisaged as elongated single-bond distances (Ru(2)–Ru(1) = 3.026 (1) Å, Ru(2)–Ru(3) = 2.956 (1) Å) while the third one has a normal single-bond distance (Ru(1)–Ru(3) = 2.793 (1) Å). These values may be compared with the Ru–Ru single-bond lengths found in $Ru_3(CO)_{12}$, which are 2.854 (3) Å (mean).[14] In the 48e trinuclear species $Ru_3(CO)_8$(*neo*-Pent–DAB), Ru–Ru distances are found between 2.737 (1) and 2.825 (1) Å, all considered as normal bond lengths.[15] All nine carbonyls in $Ru_3(CO)_9$(c-Hx–DAB) are terminally bonded: four to Ru(3), three to Ru(2), and two to Ru(1). Ru(2) is approximately octahedrally surrounded by N(1), N(2), C(23), and C(22), which are almost in one plane (maximum deviation 0.01 Å), while Ru(2) deviates only 0.17 Å from this plane. The Ru(2)–C(21) and the Ru(2)–Ru(3) vectors are both about perpendicular to the above-mentioned plane (88.9 and 86.2°, respectively). Ru(3), which bridges the Ru(1)–Ru(2) bond, also has a distorted octahedral coordination, and the geometry in the Ru(3)$(CO)_4$ unit closely resembles that of the three Ru$(CO)_4$ units in $Ru_3(CO)_{12}$.[14] C(33) and C(34) are almost in one plane with the three Ru atoms, and the C(31)–C(32) vector is perpendicular to this plane. The average Ru(3)–C(carbonyl) distance of 1.93 (1) Å is comparable to that of 1.932 (4) Å found in $Ru_3(CO)_{12}$.

The Ru(1)–Ru(2) bond is also bridged by the c-Hx–DAB ligand, which is bonded to Ru(2) via N(1) and N(2) (Ru(2)–N(1) = 2.122 (7) Å, Ru(2)–N(2) = 2.131 (7) Å). The four central atoms of the ligand, N(1), C(1), C(2), and N(2), are located at about equal distance (2.22 (1) Å) from Ru(1). These geometries indicate that in the present compound the c-Hx–DAB ligand is σ-N,σ-N′ coordinated to Ru(2) and η^2-C=N,η^2-C′=N′ coordinated to Ru(1).[2,5,6]

The N(1)C(1)C(2)N(2) skeleton is flat with a maximum deviation of 0.002 Å, the torsion angle between N(1)–C(1) and N(2)–C(2) being 0°. This N(1)C(1)C(2)N(2) plane is perpendicular (89.8°) to the Ru(1)Ru(2)Ru(3) plane, and Ru(2) deviates significantly from the N(1)C(1)C(2)N(2) plane with a dihedral angle between N(1)Ru(2)N(2) and the diimine plane of 21.7°. For other compounds in which an 8e-coordinated R–DAB ligand is present, significantly smaller dihedral angles have been observed [6.5° in $Ru_2(CO)_5$(*i*-Pr–DAB), 14° in $Ru_4(CO)_8$(*i*-Pr–DAB)$_2$, 10.0° in $Mn_2(CO)_6$(Me–DAB{Me,Me})], but in these compounds the diimine ligand bridges a much smaller metal–metal bond. (Cf. ref 6 and references therein.)

The two equal N=C bond lengths of 1.39 Å, the C(1)–C(2) bond length of 1.386 (11) Å, and the bond angles around the imine N and imine C atoms of about 115.0° are all indicative of an 8e, σ-N,σ-N′,η^2-C=N,η^2-C′=N′ coordination mode.[2,5,6,15] In free c-Hx–DAB the imine N and imine C atoms are purely sp^2 hybridized, as evidenced by the N=C and C—C′ bond lengths of 1.258 (3) and 1.457 (3) Å, respectively, and by the bond angles of 120.8 (2)°.[16] The extensive N=C bond lengthening in $Ru_3(CO)_9$(c-Hx–DAB) is due to π back-bonding from Ru(1) and Ru(2) to the LUMO of the diimine, which is antibonding between C and N. Moreover, the C–C′ bond length is shortened as a result of the bonding character of the LUMO between these atoms.[16] The π back-bonding results in a hybridization of the imine N and C atoms being in between sp^3 and sp^2.

The cyclohexyl rings on both imine N atoms are in the chair conformation with normal C–C distances and bond angles (see Tables IV and V).

(14) Churchill, M. R.; Hollander, F. J.; Hutchinson, J. P. *Inorg. Chem.* **1977**, *16*, 2655.
(15) Polm, L. H.; Keijsper, J. J.; van Koten, G.; Vrieze, K.; Stam, C. H., to be submitted for publication.
(16) Keijsper, J. J.; van der Poel, H.; Polm, L. H.; van Koten, G.; Vrieze, K.; Seignette, P. F. A. B.; Varenhorst, R.; Stam, C. H. *Polyhedron* **1983**, *2*, 1111.
(17) (a) Crystal structure: ref 14. (b) Crystal structure (R = c-Hx): ref 16. (c) Crystal structure analogous to that of $Fe(CO)_3$(2,6-(*i*-Pr)$_2$Ph–DAB): ref 18b. (d) Crystal structure analogous to that of $Fe_2(CO)_6$(c-Hx–DAB): ref 9. (e) Crystal structure (R = *i*-Pr): ref 6. (f) R–IAE = bis{(R–imino)(R–amino)ethane}, crystal structure analogous to that of {bis[(μ-isopropylamino)-2-pyridylmethane-*N*]}pentacarbonyldiruthenium: ref 15. (g) Crystal structure analogous to that of $Mo_2(CO)_6$(*i*-Pr–IAE): ref 17l. (h) Crystal structure (R = *i*-Pr): ref 3. (i) Crystal structure (R = *i*-Pr): ref 2. (j) Crystal structure (R = c-Hx): this report. (k) Crystal structure (R = *neo*-Pent): ref 15. (l) Staal, L. H.; Oskam, A.; Vrieze, K.; Roosendaal, E.; Schenk, H. *Inorg. Chem.* **1979**, *18*, 1634.

Discussion

Reaction Sequence. The complete $Ru_3(CO)_{12}$/R–DAB reaction sequence is outlined in Figure 2.

The formation of $Ru(CO)_3$(R–DAB) in this reaction as the first observable intermediate is based on the following considerations: First, the IR spectra (ν(CO) region) both of the initial reaction mixture and of isolated $M(CO)_3$(R–DAB)[2] (M = Ru, R = (i-Pr)$_2$Me, mesityl; M = Fe, R = t-Bu, i-Pr, c-Hx, 2,6-(i-Pr)$_2$Ph) are comparable (see also Table I). The latter $Fe(CO)_3$(R–DAB) species have been fully characterized[18] by mass and NMR spectroscopies and by a crystal structure determination of $Fe(CO)_3$(2,6-(i-Pr)$_2$Ph–DAB).[18b] Second, when a large excess of R–DAB is used, this first intermediate is rather persistent and reacts only very slowly to $Ru_2(CO)_4$(R–DAB)$_2$. It is likely, therefore, that this species is a monomer since it is known that a high ligand concentration favors cluster breakdown to monomeric species.[19,20]

$Ru(CO)_3$(R–DAB) reacts within 2 h with $Ru_3(CO)_{12}$ to give $Ru_2(CO)_6$(R–DAB) and $Ru_2(CO)_5$(R–DAB). As can be seen from Figure 2, this latter species, whose synthesis and reactivity have been described elsewhere, is the key intermediate in the reaction sequence: different products result from its further reaction not only by itself but also with R–DAB and $Ru_3(CO)_{12}$.[6]

Comparison of the Reactions of R–DAB with the Iron Triad Carbonyls. $Fe_2(CO)_9$ reacts with R–DAB according to the equation[7a]

$$Fe_2(CO)_9 + 2R\text{-}DAB \xrightarrow[-Fe(CO)_5]{-RNC(H)C(H)N(R)CO} Fe(CO)_3(R\text{-}DAB) \underset{+CO,\ +R\text{-}DAB,\ \Delta T}{\overset{+Fe_2(CO)_9,\ -CO,\ -Fe(CO)_5}{\rightleftharpoons}} Fe_2(CO)_6(R\text{-}DAB)$$

An important feature of this reaction is the quasi-catalytic formation of the CO-inserted imidazolone product.

In the reactions of $M_3(CO)_{12}$ (M = Ru, Os) with R–DAB, no formation of either imidazolone or of $M(CO)_5$ is observed and a reaction pathway, involving a $M_3(CO)_{10}$(R–DAB) intermediate, has been tentatively suggested.[2,7b] However, the reaction sequence, as outlined in Figure 2 for M = Ru, is different and is in its initial stages more analogous to the $Fe_2(CO)_9$/R–DAB reaction. In spite of the relative strength of the Ru–Ru bond, with respect to the Fe–Fe bond, in both $Ru_3(CO)_{12}$/R–DAB as well as in the $Fe_2(CO)_9$/R–DAB reaction, the parent carbonyl breaks down to give mononuclear $M(CO)_3$(R–DAB). It is, however, very likely that for M = Ru the cluster breakdown is preceded by coordination of R–DAB to the Ru_3 cluster, but this step cannot be observed. After the formation of $M_2(CO)_6$(R–DAB) out of the monomer and the parent carbonyl, the two reaction routes diverge: $Fe_2(CO)_6$(R–DAB) reacts upon heating or with R–DAB to afford the thermodynamically stable $Fe(CO)_3$(R–DAB). The formation of $Fe_2(CO)_5$(R–DAB) has never been observed so that, until now, $Fe_2(CO)_6$(R–DAB) is the only polyiron R–DAB species. $Ru_2(CO)_6$(R–DAB), however, can react further via $Ru_2(CO)_5$(R–DAB) to give a variety of cluster compounds as can be seen from Figure 2.

From the reaction of $Os_3(CO)_{12}$ with R–DAB, only $Os_2(CO)_6$(R–DAB) has been isolated but other products have been detected by HPLC.[7b] The precise $Os_3(CO)_{12}$/R–DAB reaction sequence and the reactivity of the products are now being studied.

Influence of R. The overall reaction route, depicted in Figure 2, is the same for every R–DAB, though R determines the actual thermodynamic stability of the products. In an earlier stage of our study of the Ru carbonyl R–DAB chemistry, it has been proposed that this stability depends mainly on the steric properties of R,[2] in particular on the branching at C^α and at C^β.[8a] Now that the overall reaction route is known and many more $Ru_x(CO)_y$(R–DAB)$_z$ products have been isolated, we are able to treat the relationship between the nature of R and the thermodynamic stability more definitely:

When R is doubly branched at both C^α and C^β (with respect to the imine N atom), the C=N double bonds of the ligand's skeleton are shielded, thereby destabilizing η^2-C=N coordination. Thus, $Ru(CO)_3$(R–DAB) is the only product for R = (i-Pr)$_2$Me, 2,4,6-mesityl, and 2,6-xylyl.

When R is triply branched at C^α (R = t-Bu), 6e coordination predominates and 8e coordination is scarce; thus, $Ru_2(CO)_6$(t-Bu–DAB) is relatively stable, and $Ru_2(CO)_5$(t-Bu–DAB) is formed only with great difficulty. $Ru_3(CO)_n$(R–DAB) (n = 8, 9) and $Ru_4(CO)_8$(t-Bu–DAB)$_2$ are not observed.

When R is doubly branched at C^α and not or singly branched at C^β, 6e as well as 8e coordination is observed. Thus, for R = i-Pr and c-Hx, $Ru_2(CO)_6$(R–DAB) and $Ru_2(CO)_4$(R–DAB)$_2$ as well as $Ru_4(CO)_8$(R–DAB)$_2$ and $Ru_2(CO)_5$(R–DAB) can be isolated. For R = p-Tol, only $Ru_2(CO)_4$(p-Tol–DAB)$_2$ can be isolated.

When R is singly branched at C^α, 8e coordination is favored. The branching on C^β seems to be less important, because for R = neo-Pent and R = i-Bu analogous products are found. $Ru_2(CO)_5$(R–DAB), $Ru_4(CO)_8$(R–DAB)$_2$, and $Ru_3(CO)_n$(R–DAB) (n = 8, 9) are relatively stable, and $Ru_2(CO)_6$(R–DAB) cannot be isolated.

Formation of $Ru_3(CO)_9$(R–DAB). The structures of $Ru_3(CO)_8$(R–DAB) and of $Ru_3(CO)_9$(R–DAB), found for R = neo-Pent and R = c-Hx, respectively, are schematically presented in Figure 3, together with relevant geometric properties. The diimine ligand in $Ru_3(CO)_8$(R–DAB) acts as an 8e donor, and as a consequence there are three normal single Ru–Ru bonds in this 48e species.[15]

For $Ru_3(CO)_9$(R–DAB) two possible structures were expected: first, a structure in which there would still be three Ru–Ru bonds but with R–DAB acting as a 6e-donor ligand and as a consequence the added CO molecule bonding to Ru(1);[7b] second, a structure in which one Ru–Ru bond would be broken but with R–DAB still acting as a 8e-donor ligand. However, neither of these situations is found in the actual structure of $Ru_3(CO)_9$(c-Hx–DAB) because neither a metal–metal bond nor a metal–ligand bond is broken completely.

The reaction of CO with $Ru_2(CO)_5$(R–DAB), which is isostructural with $Ru_3(CO)_8$(R–DAB) through replacement of the μ-$Ru_3(CO)_4$ unit for an isolobal μ-CO group[21] (see Figure 2), yields $Ru_2(CO)_6$(R–DAB). The Ru atoms in both initial and final products obey the 18e rule. This is made possible because during the reaction 8e, σ-N,σ-N′, η^2-C=N,η^2-C′-N′-bonded R–DAB is converted to 6e, σ-N,μ^2-N′,η^2-C=N′-bonded one, while the bridging CO group becomes terminal. In the reaction of $Ru_3(CO)_8$(R–DAB) with CO, such a rearrangement is not possible because of the presence of the μ-Ru(3)$(CO)_4$ unit, which unlike CO cannot act as a single-bonded moiety. As a consequence, 50e $Ru_3(CO)_9$(R–DAB) does not obey the 18e rule.

As can be seen from Figure 3, the geometry around Ru(2) suggests that addition of CO to $Ru_3(CO)_8$(R–DAB) can occur because there is an empty site, trans to Ru(3), in the coordination sphere of Ru(2) (see also Results and Table V). As a result of this addition, the electron density on Ru(2) will increase and simple electron counting, on the assumption of σ-N,σ-N′ coordination of R–DAB to Ru(2) and normal 2e metal–metal bonds, indeed leads to 20 valence electrons on Ru(2). Figure 3 also shows that upon going from the octa- to the nonacarbonyl the overall structure is hardly changed. The most striking effects that show how the cluster reacts on the electron input are situated around Ru(2) and are as follows:

Ru(2)–Ru(n) (n = 1, 3) are both lengthened by 0.2 Å, indicating that the electron density is partly moved to an antibonding

(18) (a) Otsuka, S.; Yoshida, T.; Nakamura, A. *Inorg. Chem.* **1967**, *6*, 20. (b) Kokkes, M. W.; Stufkens, D. J.; Oskam, A. *J. Chem. Soc., Dalton Trans.* **1983**, 439 and references therein.

(19) See e.g.: Deeming, A. J. "Transition Metal Clusters"; Johnson, B. F. G., Ed.; 1980.

(20) Chisholm, M. H.; Rothwell, I. P. *Prog. Inorg. Chem.* **1982**, *29*, 1.

(21) Evans, D. G. *J. Chem. Soc., Chem. Commun.* **1983**, 675 and references cited therein.

metal–metal orbital, localized mainly on Ru(2). The Ru(1)–Ru(3) distance is hardly affected (2.737 → 2.793 Å). In other trinuclear clusters, a large metal–metal bond length is normally due[22] to either the presence of a bridging hydride[23] or the steric requirements of a bridging ligand, as found in, e.g., $Ru_3(CO)_9[MeSi(PBu_2)_3]$[24] and in trinuclear azulene or pentalene complexes.[25] R–DAB, however, can easily bridge a Ru–Ru bond of 2.741 Å, as found in $Ru_2(CO)_5$(*i*-Pr–DAB). Thus, the long Ru(1)–Ru(2) distance in $Ru_3(CO)_9$(c-Hx–DAB) is not sterically demanded.

The three carbonyls on Ru(2) in $Ru_3(CO)_9$(R–DAB) are more weakly bonded than the two carbonyls on Ru(2) in $Ru_3(CO)_8$(R–DAB). This can be concluded from the average Ru(2)–C(carbonyl) bond length, which increases from 1.83 (1) Å in $Ru_3(CO)_8$(*neo*-Pent–DAB) to 1.91 (1) Å in $Ru_3(CO)_9$(c-Hx–DAB), the "new" Ru(2)–C(21) bond having the largest distance of 1.925 (8) Å. Indeed, $Ru_3(CO)_9$(R–DAB) easily loses CO to give $Ru_3(CO)_8$(R–DAB) (see Results). The Ru(*n*)–C(carbonyl) (*n* = 1, 3) distances are not affected.

There is a general rule that says when a 2e-donor ligand is added to a polynuclear species, one observes either dissociation of a metal–ligand bond or metal–metal bond breaking.[20,26] An example of the first possibility is found in the reaction of $Mn_2(CO)_5(Ph_2PCH_2PPh_2)$ with CO, yielding $Mn_2(CO)_6(Ph_2PCH_2PPh_2)$, a reaction in which 4e-coordinated CO is converted to 2e-coordinated CO.[27] The other possibility is found, e.g., in the reactions of trinuclear $MnFe_2$ clusters with P ligands or CO, when a Mn–Fe bond is broken.[28a] Yet another example of this latter possibility is found in the reaction of $M_3(CO)_8(C{\equiv}CR)(PPh_2)$[28b] (M = Ru, Os; R = *i*-Pr, *t*-Bu) with CO. During this reversible reaction, one M–M bond is broken and re-formed again when CO dissociates from the nonacarbonyl product. As a consequence, formally 50e trinuclear clusters contain only two metal–metal bonds as is indeed found in $Ru_3(CO)_{10}(NO)_2$,[29] $Ru_3(CO)_8(C_9H_6NO)_2$,[30] $Os_3(CO)_{10}(OMe)_2$,[31] $Ru_3(CO)_9(C{\equiv}C\text{-}i\text{-}Pr)(PPh_2)$,[28b] and $Fe_3(\mu_3\text{-}S)_2(CO)_9$[22] where two metal–metal separations are considered as normal bonding interactions and one longer separation is described as a nonbonding interaction. This rule, which is a consequence of the 2e–2c description, almost never fails for trinuclear clusters[32] but is not always valid for higher nuclearity clusters. In 64e tetranuclear clusters, for example, in which four metal–metal bonds are expected, one sometimes finds five metal–metal bonds of which two or three have a bond order less then 1.[33]

Recently, several theories have been developed to describe these types of clusters.[34] One of these, i.e. the polyhedral skeletal electron pair theory (PSEPT), has been rather successful in relating the geometry of the more simple cluster to the stoichiometry.[36] Furthermore, this theory can be rather readily applicated, and main-group atoms may easily be treated as cluster units. On the other hand, however, it fails when vacant s, p, or d cluster valence molecular orbitals (CVMO) are present.[37] In the present case the PSEPT can be used to explain the structure of $Ru_3(CO)_9$(c-Hx–DAB), which does not fit the 18e rule (vide supra). Also, the analogy, which does not exist with normal electron-counting procedures, between the reactions of $Ru_2(CO)_5$(R–DAB) and of $Ru_3(CO)_8$(R–DAB) with CO then becomes apparent. According to this theory and by treatment of the C(H) and N(R) units of the ligand as 3e- and 4e-contributing vertices, respectively, both $Ru_2(CO)_5$(R–DAB) and $Ru_3(CO)_8$(R–DAB) are found to be nido-type clusters. Both are based on a pentagonal bipyramid, containing eight skeletal electron pairs. One edge of the polyhedron is bridged by a CO or a $Ru(CO)_4$ unit, respectively. Reaction of these species with CO yields the arachno-type clusters $Ru_2(CO)_6$(R–DAB) and $Ru_3(CO)_9$(R–DAB), respectively. The structure of the former, containing a 6e-bonded ligand, can easily be fitted into a dodecahedron. However, the latter structure, containing an 8e-bonded ligand, may be also thought of as based on a dodecahedron, though a distorted one.

According to the CVMO theory, the octacarbonyl compound is a normal three-atom cluster, having accordingly 24 filled CVMOs. Evidently, one HLAO (highly lying antibonding orbital)[37] is so low lying that it can be occupied by CO ligand electrons. In the resulting nonacarbonyl species, only two HLAOs will be present, resulting not in metal–metal bond breaking but in overall weakening of the metal–metal bonds.

Conclusions

$Ru_3(CO)_{12}$ reacts with R–DAB in a reaction sequence that involves complete cluster breakdown. After the formation of $Ru(CO)_3$(R–DAB) di- and polynuclear species are formed.

Reversible addition of a 2e-donor CO ligand to a 48e trinuclear Ru species is possible, without the complete rupture of bonds. The extra electrons are mainly localized around one Ru(2) atom, weakening not only the two Ru(2)–Ru(*n*) (*n* = 1, 3) but also all Ru(2)–C(carbonyl) bonds, which is a rather unique feature. Other parts of the molecule are hardly affected. Therefore, the green–red color change during the reaction is presumably the result of the change in coordination of Ru(2).

The 50e $Ru_3(CO)_9$(R–DAB) can be described as the first trinuclear Ru cluster, because it cannot be interpreted on basis of the 18e rule but fits rather well in the PSEPT. On the basis of this theory, reactions of $Ru_2(CO)_5$(R–DAB) and of $Ru_3(CO)_8$(R–DAB) with CO are analogous.

(22) A trinuclear species with one extra electron in an antibonding metal–metal orbital is 49e $Co_3(CO)_9(\mu_3\text{-}S)$. The extra electron weakens all Co–Co bonds: Wei, C. H.; Dahl, L. F. *Inorg. Chem.* **1967**, *6*, 1229.

(23) (a) Raithby, P. R. "Transition Metal Clusters"; Johnson, B. F. G., Ed.; Wiley-Interscience: New York, 1980. (b) Lavigne, G.; Lugan, N.; Bonnet, J. J. *Organometallics* **1982**, *1*, 1040 and references cited therein.

(24) de Boer, J. J.; van Doorn, J. A.; Masters, C. *J. Chem. Soc., Chem. Commun.* **1978**, 1005.

(25) (a) Howard, J. A. K.; Stansfield, R. F. W.; Woodward, P. J. *J. Chem. Soc., Dalton Trans.* **1979**, 1812. (b) Churchill, M. R.; Wormald, J. *Inorg. Chem.* **1973**, *12*, 191.

(26) Johnson, B. F. G.; Raithby, P. R.; Zuccaro, C. *J. Chem. Soc., Dalton Trans.* **1980**, 99.

(27) Wolff, T. E.; Klemann, L. P. *Organometallics* **1982**, *1*, 1667.

(28) (a) Schneider, J.; Huttner, G. *Chem. Ber.* **1983**, *113*, 917. (b) Carty, A. J.; Maclaughlin, S. A.; Taylor, N. J. *J. Organomet. Chem.* **1981**, *204*, C27.

(29) Norton, J. R.; Collman, J. P.; Dolcetti, G.; Robinson, W. T. *Inorg. Chem.* **1972**, *11*, 382.

(30) van Doorn, J. A.; van Leeuwen, P. W. N. M. *J. Organomet. Chem.* **1981**, *222*, 299.

(31) Allen, V. F.; Mason, R.; Hitchcock, P. B. *J. Organomet. Chem.* **1977**, *140*, 297.

(32) (a) To our knowledge three trinuclear clusters are known containing more than 48 skeleton electrons and that have short metal–metal distances: $Co_3(CO)_9(\mu_3\text{-}PPh)$, $Co_3(CO)_4(\mu\text{-}SEt)_5$, and $Rh_3(CO)_4(\mu\text{-}PPh_2)_3(\mu\text{-}Cl)_2$. Haines, R. J.; Steen, N. D. C. T.; English, R. B. *J. Chem. Soc., Dalton Trans.* **1983**, 2229 and references cited therein. (b) There are some examples in which a trinuclear cluster contains more than 48 electrons and in which all metal–metal bonds are weakened. See e.g.: Frisch, P. D.; Dahl, L. F. *J. Am. Chem. Soc.* **1972**, *94*, 5082 and references therein. See also ref 22.

(33) (a) In $FeRu_3(CO)_{13}(\mu\text{-}PPh_2)_2$, having a planar butterfly-like geometry, the three Ru–Ru separations are about 3.1 Å and have a bond order of $^2/_3$: Churchill, M. R.; Bueno, C.; Young, D. A. *J. Organomet. Chem.* **1981**, *213*, 139. (b) In 64e $Os_4(CO)_{12}(\mu_3\text{-}S)_2$, having a butterfly arrangement of the Os_4 unit with the sulfido ligands bridging the "open" triangular faces, two weak and three normal Os–Os interactions are found: Adams, R. D.; Yang, L. W. *J. Am. Chem. Soc.* **1982**, *104*, 4115; **1983**, *105*, 235.

(34) For a new topological electron-counting theory for high-nuclearity clusters and for a survey of other (semi)empirical theories, see: Teo, B. K. *Inorg. Chem.* **1984**, *23*, 1251 and the references 1–15 therein.

(35) Wade, K. In "Transition Metal Clusters"; Johnson, B. F. G., Ed.; Wiley-Interscience: New York, 1980.

(36) See e.g.: Adams, R. D.; Horvath, I. T.; Mathur, P. *Organometallics* **1984**, *3*, 623. Adams, R. D.; Horvath, I. T.; Mathur, P.; Segmueller, B. E.; Yang, L. W. *Ibid.* **1983**, *2*, 1078. Adams, R. D.; Yang, L. W. *J. Am. Chem. Soc.* **1982**, *104*, 4115.

(37) Lauher, J. W. *J. Organomet. Chem.* **1981**, *213*, 25.

Acknowledgment. We thank D. Heijdenrijk for collecting the X-ray data, R. Fokkens for recording the mass spectra, and J. M. Ernsting for recording the 250-MHz NMR spectra. We thank the Netherlands Foundation for Chemical Research (S.O.N.) and The Netherlands Organization for Pure Research (Z.W.O.) for their financial support.

Registry No. $Ru(CO)_3$(R-DAB) (R = *i*-Pr), 94249-99-7; $Ru(CO)_3$(R-DAB) (R = c-Hx), 94250-00-7; $Ru(CO)_3$(R-DAB) (R = *i*-Bu), 94250-01-8; $Ru(CO)_3$(R-DAB) (R = *neo*-Pent), 94250-02-9; $Ru(CO)_3$(R-DAB) (R = *p*-Tol), 94250-03-0; $Ru_2(CO)_6$(R-DAB) (R = *i*-Pr), 94278-61-2; $Ru_2(CO)_6$(R-DAB) (R = c-Hx), 94250-04-1; $Ru_2(CO)_5$(R-DAB) (R = *i*-Bu), 94250-05-2; $Ru_2(CO)_5$(R-DAB) (R = *neo*-Pent), 94250-06-3; $Ru_2(CO)_4$(R-DAB)$_2$ (R = *p*-Tol), 94250-07-4; $Ru_2(CO)_4$(R-DAB)$_2$ (R = *i*-Bu), 94250-08-5; $Ru_2(CO)_4$(R-DAB)$_2$ (R = *neo*-Pent), 94294-07-2; $Ru_3(CO)_9$(R-DAB) (R = *neo*-Pent), 94278-62-3; $Ru_3(CO)_9$(R-DAB) (R = *i*-Bu), 94250-09-6; $Ru_3(CO)_8$(R-DAB) (R = *neo*-Pent), 94250-11-0; $Ru_3(CO)_8$(R-DAB) (R = *i*-Bu), 94250-12-1; $Ru_3(CO)_9$(R-DAB) (R = c-Hx), 94250-10-9; $Ru_3(CO)_{12}$, 15243-33-1.

Supplementary Material Available: Listings of analytical data and anisotropic thermal parameters, Figure 4 showing IR spectra, and listings of observed and calculated structure factors and bond distances (24 pages). Ordering information is given on any current masthead page.

Contribution from the Department of Chemistry and Laboratory for Molecular Structure and Bonding, Texas A&M University, College Station, Texas 77843, and Department of Chemistry and Biochemistry, Southern Illinois University, Carbondale, Illinois 62901

A Novel d^{10}–d^3–d^{10} Trinuclear Bimetallic Linear Complex of Zinc and Vanadium

F. ALBERT COTTON,*[1a] STAN A. DURAJ,[1a] WIESLAW J. ROTH,[1a] and C. DAVID SCHMULBACH*[1b]

Received May 31, 1984

The reaction of $[V_2(\mu\text{-}Cl)_3(THF)_6]_2[Zn_2Cl_6]$ with triphenylphosphine in benzene furnishes $[V_2(\mu\text{-}Cl)_3(THF)_5(PPh_3)]_2[Zn_2Cl_6]$, which in turn gives $(PPh_3)(Cl)Zn(\mu\text{-}Cl)_2(THF)V(THF)(\mu\text{-}Cl)_2Zn(Cl)(PPh_3)$ upon treatment with dichloromethane. The mono(triphenylphosphine) derivative was characterized by elemental analysis and X-ray fluorescence measurements. The V-$[Zn(Cl)_3(THF)(PPh_3)]_2 \cdot 2CH_2Cl_2$ molecule was fully characterized by single-crystal X-ray studies. The data are as follows: triclinic space group, $P\bar{1}$, a = 11.922 (3) Å, b = 14.189 (2) Å, c = 8.991 (3) Å, α = 107.47 (1)°, β = 108.03 (2)°, γ = 86.16 (1)°, V = 1379 (1) Å^3, Z = 1. The principal structural features of interest are as follows: Zn–V distance of 3.289 (1) Å; Zn–P distance of 2.392 (1) Å; Zn–Cl distances of 2.324 (1) and 2.293 (1) Å for $Zn\text{-}Cl(2)_b$ and $Zn\text{-}Cl(3)_b$, respectively, and of 2.197 (1) Å for $Zn\text{-}Cl(1)_t$.

Introduction

$[V_2(\mu\text{-}Cl)_3(THF)_6]_2[Zn_2(\mu\text{-}Cl)_2Cl_4]$,[2] previously known in the literature as $VCl_2(THF)_2$, represents an interesting starting material for entry into the nonaqueous chemistry of lower valent vanadium complexes. Under certain conditions it leads to compounds that contain vanadium only, e.g., $V_3(\mu_3\text{-}O)(CF_3CO_2)_6(THF)_3$[3] or $[VCl(dppm)BH_4]_2$,[4] but it can also give rise to unusual vanadium- and zinc-containing metal complexes such as $[VZnO(C_6H_5CO_2)_3(THF)]_4 \cdot 2THF$[5] or $[VZnH_2(BH_4)(PMePh_2)_2]_2$.[6] In this paper we report another example of a bimetallic compound, with some unusual features of interest, that was obtained from $[V_2Cl_3(THF)_6]_2[Zn_2Cl_6]$, albeit by a two-step procedure. This novel linear complex, $(PPh_3)(Cl)Zn(\mu\text{-}Cl)_2(THF)V(THF)(\mu\text{-}Cl)_2Zn(Cl)(PPh_3) \cdot 2CH_2Cl_2$ provides a rare example of a zinc complex containing phosphine ligands.

Experimental Section

All operations were performed under an atmosphere of argon by using standard Schlenk techniques and a double-manifold vacuum line. Solutions and solvents were transferred via stainless cannulae and/or syringes. Dichloromethane was freshly distilled from P_2O_5, and benzene and hexane were distilled from benzophenone ketyl prior to use. Triphenylphosphine was deaerated under vacuum at room temperature. $[V_2(\mu\text{-}Cl)_3(THF)_6]_2[Zn_2Cl_6]$ was prepared according to the published procedure.[2] Elemental analyses were performed by Galbraith Microanalytical Laboratories. Source-excited X-ray fluorescence analysis was done with a 100-mCi ^{241}Am excitation source. X-rays emitted from the sample were detected and analyzed on a KEVEX lithium-drifted silicon detector [Si(Li)]. Detector output pulses were digitized and evaluated with a Nuclear Data ND66 pulse height analyzer. We thank Professor E. Schweikert of this department for the X-ray fluorescence analysis.

Table I. Summary of Crystallographic Data

formula	$Zn_2VCl_{10}P_2O_2C_{46}H_{50}$
fw	1233.07
space group	$P\bar{1}$
a, Å	11.922 (3)
b, Å	14.189 (2)
c, Å	8.991 (3)
α, deg	107.47 (1)
β, deg	108.03 (2)
γ, deg	86.16 (1)
V, Å^3	1379 (1)
Z	1
d_{calcd}, g/cm^3	1.485
cryst size, mm	0.3 × 0.6 × 0.6
μ(Mo Kα), cm^{-1}	16.261
data collcn instrum	Syntex $P\bar{1}$
radiation (monochromated in incident beam)	Mo Kα (λ = 0.710 73 Å)
orientation reflcns: no.; range (2θ), deg	15; 18.14 ≤ 2θ ≤ 31.18
temp, °C	20
scan method	ω–2θ
data collecn range (2θ), deg	4 ≤ 2θ ≤ 50 ($+h, \pm k, \pm l$)
no. of unique data; total with $F_o^2 > 3\sigma(F_o^2)$	3770; 3094
no. of parameters refined	283
transmissn factors: max, min	0.999, 0.8840
R^a	0.0545
$R_w{}^b$	0.0820
quality-of-fit indicator[c]	1.796
largest shift/esd, final cycle	0.061
largest peak, e/Å^3	1.161[d]

[a] $R = \Sigma||F_o| - |F_c||/\Sigma|F_o|$. [b] $R_w = [\Sigma w(|F_o| - |F_c|)^2/\Sigma w|F_o|^2]^{1/2}$; $w = 1/\sigma^2(|F_o|)$. [c] Quality of fit = $[\Sigma w(|F_o| - |F_c|)^2/(N_{observns} - N_{parameters})]^{1/2}$. [d] Located in the vicinity of the disordered CH_2Cl_2 molecule; the second largest peak with intensity 0.725 e/Å^3.

$[V_2(\mu\text{-}Cl)_3(THF)_5PPh_3]_2[Zn_2Cl_6]$. To a slurry of $[V_2Cl_3(THF)_6]_2[Zn_2Cl_6]$ (2.5 g, 1.5 mmol) in 20 mL of benzene, prepared in a 100-mL

(1) (a) Texas A&M University. (b) Southern Illinois University
(2) Cotton, F. A.; Duraj, S. A.; Extine, M. W.; Lewis, G. E.; Roth, W. J.; Schmulbach, C. D.; Schwotzer, W. *J. Chem. Soc., Chem. Commun.* **1983**, 1377.
(3) Cotton, F. A.; Lewis, G. E.; Mott, G. N. *Inorg. Chem.* **1982**, *21*, 3316.
(4) Cotton, F. A.; Duraj, S. A.; Roth, W. J. *Inorg. Chem.* **1984**, *23*, 4113.
(5) Cotton, F. A.; Duraj, S. A.; Roth, W. J. *Inorg. Chem.* **1984**, *23*, 4042.
(6) Bansemer, R. L.; Huffman, J. C.; Caulton, K. G. *J. Am. Chem. Soc.* **1983**, *105*, 6163.

0020-1669/85/1324-0525$01.50/0